

Magnetically Actuated Minimally Invasive Microbots for Biomedical Applications

Hritwick Banerjee, Shen Shen and Hongliang Ren

Abstract This chapter elucidates comprehensive overview of magnetically actuated microbots for various biomedical applications, discover recent developments and show a possible future scope and challenges therein. We confine our biomedical applications and present state of the art mostly related to translational research and near term deliverable possibilities to make *in vivo* applications. We will first demonstrate a brief overview of the potential medical applications and recent state of the art magnetically actuated microbots. After that, we will briefly touch upon various aspects of magnetically driven magneto-responsive microcapsules for targeted Drug Delivery (TDD) applications. In this part, we will provide a brief literature review in the nexus of magnetic micro robotics with design specifications for drug delivery. Finally, we will illustrate magnetically manipulated self-propelled microjets for biosensing as future perspectives.

1 Introduction

Microbots that are associate with molecular machine have given birth to a new paradigm in biomedicine and healthcare as indicated by 2016 Nobel Prize in Chemistry to Nanomachines [25, 66]. The governing challenges now and the major point of consideration is how to power these molecular devices so that they can be used as *in vitro* molecular diagnosis and biochemical assays as well as interacting with human body *in vivo* [68]. Powering these microbots is a nontrivial challenge typically boiling down to (1) on-board supply, (2) Energy harvesting, and (3) Energy or power transmission. As many biomedical applications inside human bodies will be for intervention delivery, surgery delivery, targeted drug delivery (TDD), separations, cell sorting, and biosensing, the power and the mechanical motion are ideal to be transmitted wirelessly.

H. Banerjee · S. Shen · H. Ren (✉)
Department of Biomedical Engineering, National University of Singapore,
Singapore, Singapore
e-mail: ren@nus.edu.sg

The wireless motion and power transmission approach that we will cover in this chapter, is to use magnetic fields. Researchers in magnetically actuated self-propelled micro/nanomachines have started to apply this technology in many new avenues from biosensing, microfluidics, robotics, and environmental fields with many others [96, 97]. As for example, self-propelled microrobots [55] using closed loop control algorithm in a fluidic microchannel (Width: $500\ \mu\text{m}$, Depth: $300\ \mu\text{m}$) are believed to be integrated further for targeted drug delivery (TDD), separations, cell sorting, and biosensing applications [90, 100]. Here, self-propelled microjets used microfluidic confinement with flow rate of $0\text{--}7.5\ \mu\text{L}/\text{min}$ (for and against the flow mimicking blood circulation) [55, 63, 83, 85] in line with the consideration that microfluidic channels mimic the confinement effects induced by micro confinements of downstream physiological pathways [6]. Moreover, U-turn [3, 52] and the rotating magnetic field technique [113] characterization implemented in [55] to determine average magnetic dipole moment poses inconsistencies as: (i) Hydrogen peroxide and water dynamic viscosities are assumed to be comparable but not same (H_2O_2 viscosity: $1.245\ \text{cP}$ and Water viscosity: $1\ \text{cP}$ at 20°C) [103], while bubble dynamics incorporation is nontrivial for further development of robust self-propelled microjet magnetic setup (ii) rotating magnetic field is an optimal choice but time consuming. There is significant research where magnetically driven biomedical microbots used their helical flagella rotating like a cork screw to move onward and backward in a viscous fluid mimicking human blood circulatory systems [27]. For future research, it is hypothesized that ultrasound (US) can even be integrated with imaging and generating acoustic waves simultaneously for sonoporation and TDD incorporating established self-propelled catalytic decomposed oxygen bubbles [8, 9, 55, 58]. Further developments incorporating magnetic actuation and ultrasound guidance methods could manipulate swarms of micro robotic agents and magnetic catheters. In this regard, study in [123] uses ultrasound driven propulsion mechanism in micro/nanoscale in fuel-driven and fuel-free conditions. Conclusively, although there are studies to implement magnetically driven microbots for different biomedical applications we are still facing significant challenges for implementing the state of the art technique in real-life applications. Therefore, substantial effort needs to be established for characterizing new propulsion mechanism based on closed loop feedback control framework [124].

2 Potential Impact of Magnetically Induced Medical Microbots

The transition from macro to micro scale robotics follows fundamental law of physics but the scale length provides a sense of priority and disturbances comparing to macro scale. As for example, in micro robotics the surface to volume ratio, surface tension, and viscosity effect predominantly exhibit main counter stones in making a perfect actuation. To illustrate more, to function in the human circulatory system, a microbot

must overcome the challenges of varying diameter of blood vessel (a couple of centimeters for Aorta down to several microns in capillaries) [74] and pulsatile flow of blood in contrary to its tethered counterparts. Therefore, in order to apply magnetically driven microrobot for TDD applications, the prospective system has to pass at least three main challenges (1) the ability to continually monitor propulsion force so that the microrobot can maintain its movement against time varying blood flow inside human body (2) along with magnetic control there has to be a provision for imaging modality which will further provide the motion control of microrobot and (3) the magnetically driven micromotor control system need to be robust enough to counter balance the deviation like time varying flow, viscosity, and many others. All these challenges need to be overcome before this microbot can be used in biomedical applications.

2.1 Potential Medical Application Areas

As we discussed earlier, due to the challenges medical microbots are still far from reality. Therefore, in this section, we will illustrate the near term feasible microbots application converging to biomedical fields with relevant literature focussed on electromagnetic actuations.

2.1.1 The Blood Circulatory System

The benefits of minimally to noninvasive surgery (MIS) includes less operative pain, truncated hospitalization cost, reduced recovery period, and many others. Therefore, there are huge scientific discourses in the realm of medical trials to work on electromagnetically driven jet pumps in human circulatory systems [93]. In this paradigm, a magnetic resonance imaging (MRI) based control mechanism for micro particle tracking inside human circulatory systems *in vivo* [73, 93] proved that microparticle tracking and control against blood flow is possible with several challenges to overcome.

2.1.2 The Central Nervous System (CNS)

In the recent past, an investigation was established for successful trials of remotely controlled and guidance of magnetic seeds in the brain and several prototype systems have been developed [33, 34, 77, 78]. There was a carry forward research where the amount of forces required for the magnetic seeds were investigated within a human brain [82]. With the advent of MEMS fabrication for neurosurgery [92] in the distant future a bridge can be overlaid where magnetically driven wireless microbot can further be incorporated in neurosurgery. In this regard, noninvasive control of

microbot for endoscopy in the subarachnoid space of the spine [60] lay out a platform for future researches to investigate in this realm.

2.1.3 The Urinary System and the Prostate

Urolithiasis causes blockage of the ureter resulting in painful urination with blood and if untreated tissue damage with renal dysfunction can occur. It is a multi-factorial disorder with ever increasing prevalence leading to a disproportionate misery in human life and morbidity worldwide [35, 61]. The advancement in biomedical engineering and medical devices cemented the necessity for microbots to treat kidney stone diseases (KSD) by optimal access to the stone sites. In this regard, a biopolymer coated microbot can swim up the ureter to crush kidney stones with least harms and side effects [23]. In addition, the microbot can also be administered as a soluble capsule for temperature, pressure and pH sensor *in vivo* for long-term bladder monitoring. On the other hand, as discussed in the earlier section the advancements of MEMS (Micro-Electro-Mechanical Systems) and NMES (Nano-Electro-Mechanical Systems) devices can be integrated with wireless microbots for applications in urology [62] and allied fields.

Nowadays prostate cancer has become an epidemic such that millions of males encounter a prostate biopsy yearly only in USA. The lone available treatment now is to use an insertion needle through the perineum, during which 20% of the prostate cancer tumors are missed [19, 88, 114]. Another feasible option is to gain access through colon but at the cost of much complex maneuver and a much-controlled manipulation. Therefore, in this regime, microbots can take a huge step forward to minimize the complexity of guide wires and will produce less infections. At the same time, the microbot can carry radioactive seed to various distributed tumor locations for delivery of radiation dosage. There is an alternate path through urethra for delivering microbot to the desired prostate cancer tumor regions. The use of magnetically controlled microbots will significantly cut down the possibility of nerve damage, and noninvasive treatment will induce altogether a new paradigm of TDD [130].

2.1.4 The Eye

Despite sufficient efforts in optimizing ocular drug delivery, the progress in this domain is still in infancy in comparison to other delivery routes such as oral, transdermal, and transmucosal. Though a small volume of drug is required, to achieve the same amount using a dropper is extremely difficult to design. In addition to this, patients usually are unable to absorb small concentration of drugs required. These factors resulted in transcorneal absorption of 1% or less when applied as a solution [94] (Fig. 1). Conclusively, the amount of loss of drugs from the eyes vary 500–700 times the rate of absorption into the anterior chamber [17]. In this realm, microbots

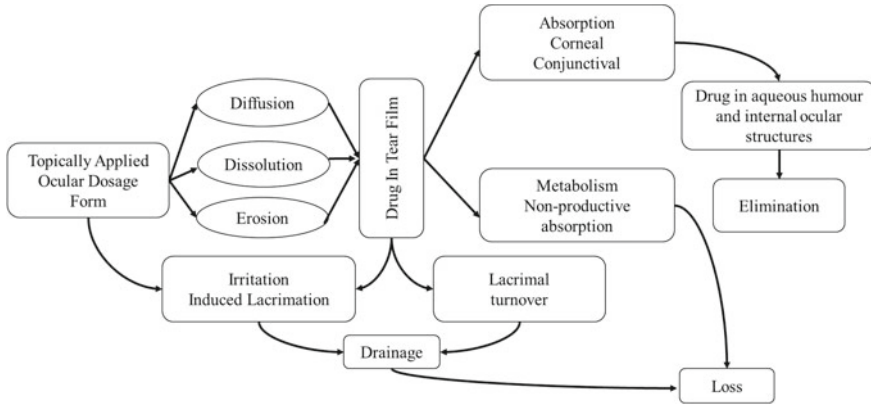


Fig. 1 Schematic illustration of the ocular disposition of topically applied constructions.

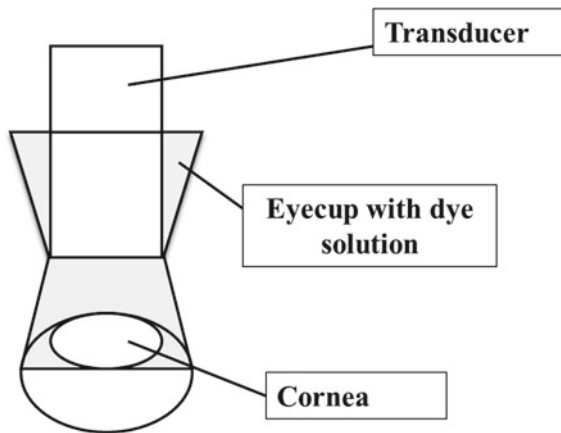


Fig. 2 A sample figure for effective ocular drug delivery.

robots can be interfaced for controlled drug delivery from anterior to posterior chambers [111].

With ever increasing advances of wirelessly controlled magnetic field, there are scientific reports where microbots have been used for intraocular procedures while tracking was possible through the pupil [129]. On the other hand, a controlled retinal therapy using magnetic microparticle tracking emerged for optimal drug delivery [42] (Fig. 2). Despite the current advances, challenges related to biocompatibility and toxicity issues need to be overcome before successful clinical trials.

2.1.5 The Fetus

Presently, 0.6–1.9% of the world population is suffering badly from Congenital Cardiovascular Malfunctions (CCM) [40]. CCM is causing birth defects, which ultimately turns into death [128]. The time of CCM detection by fetal ultrasound [28], abnormalities were already stabilized instigating progressive challenge to repair them in general. It is reported in an animal study which explains any alteration of amniotic fluid especially deficiency or low volume may be one of the causes of CCM [41, 45].

Fetal surgery is in its preliminary stage with minimum success rates and few organizations practicing it, though promising [59, 118]. In the future, micro robots,

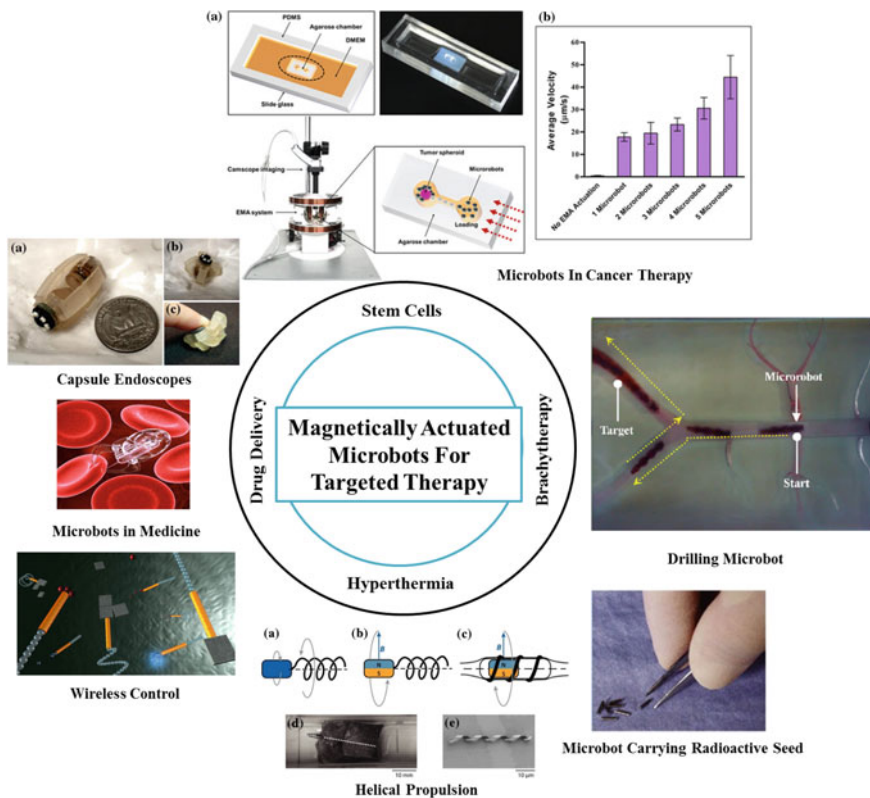


Fig. 3 Potential magnetically actuated microrobots in various medical application areas such as (i) Drug Delivery, (ii) Hyperthermia, (iii) Brachytherapy, and (iv) Stem cells research. (i) In targeted drug delivery, there are cases where soft, squishy bot controlled wirelessly used for capsule endoscope passing through human vessel. (ii) In hyperthermia treatment, microrobots optimally controlled can be used for helical propulsion where body tissue will be exposed to rise in temperature (iii) In brachytherapy, microrobots wirelessly controlled used for carrying radioactive seeds in treating tumor. (iv) In stem cells research, microrobots controlled in noninvasive manner are used for cell motility enhancement and increasing potential for cancer therapy [14, 29–31, 36, 49, 50, 64, 85, 99, 117].

can be replacements to the current techniques as researchers are developing new concepts of the minimally invasive fetal surgical system. For example, procedures to insert microbots through the cervix to uterus [7, 26]. It can clear the obstruction of the urinary tract in the fetus, in cases of congenital cystic adenomatous malformation, microbots can remove extra tissues and prevent hydrops and procedures of amniocentesis and cordocentesis can go needless with the use of microbots. Figure 3 shows potential magnetically actuated microrobots in various medical application areas such as (i) Drug Delivery, (ii) Hyperthermia, (iii) Brachytherapy, and (iv) Stem cells research.

3 Magnetically Driven Magneto-Responsive Microcapsules for Targeted Therapy

The microcapsule fabrication processes are based on the principles of calcium alginate gelation. The microcapsules are generated in bulk by encapsulation. This section is going to elucidate the following points briefly: First, the setup of the microcapsule fabrication system is described; secondly, the chemical principles of the gelation processes are introduced and finally, the detailed fabrication methodology is discussed for the three calcium alginate microcapsule designs.

In contrary to the magnetic nano particles, larger particle in microns (e.g., agglomerates of superparamagnetic microspheres, 1 micron in diameter) are more effective in sustaining with the flow dynamics of the human circulatory system—mostly in larger aortic veins and arteries (Fig. 4). Like rolling down a steep hill, the steeper the gradient is, the total force will be placed on the particle. Table 1 gives typical B field values and gives a sense of what values are realizable for a working magnetically controlled microsphere guidance system.

Table 1 Typical B field values for retention at flow speeds corresponding to capillary blood flow [105].

Distance of flow tube center from pole face (cm)	Local magnetic field strength (Oe)	Local magnetic field strength gradient (Oe/cm)	Observed particle retention (%)	Longitudinal flow speed, computed for full retention (cm/sec)
1.0	1150	770	99	0.207
1.9	670	370	98	0.095
2.7	460	170	26	0.039
4.6	240	66	14	0.015

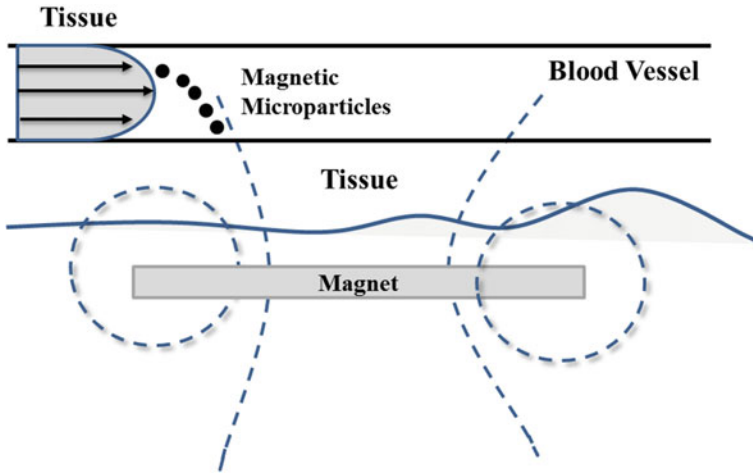


Fig. 4 A concept of magnetic actuated drug delivery system. The magnets or electromagnetic coils positioned optimally outside the body so that the generated magnetic field will influence the magnetic-responsive micro particles inside the blood vessel for manipulation and control [32, 86].

3.1 Design of Magneto-Responsive Microcapsules

3.1.1 General Mechanism of B-390 Encapsulation

Generally, the B-390 Encapsulator is a machinery that utilizes the charged vibration nozzle to generate droplets of the liquid flowing through it. As illustrated in Fig. 5, after the liquid is pumped in with a syringe pump, it is vibrated into small droplets, where the frequency is selectable between 0–6000 Hz. The droplets are charged by an electric field, which is selectable between 0–2500 V at the same time. The charged droplets are dispersed because they possess the same charge, then fall into the coagulation solution for gelation [16, 104].

Figure 5 presents the mechanism of the Encapsulator B-390 and step by step procedure for encapsulation. Here, Step 1 is mixing of active ingredient and polymer while Step 2 signifies pumping of mixture with syringe pump or air pressure. Step 3 defines superimposition of vibration and Step 4 is the droplet formation. After droplets accumulate Electrostatic charge dispersion followed as demonstrated in Step 5. Thereafter, Step 6 defines the online process control of droplet formation in the light of the stroboscope lamp and Step 7 proposes Bead formation in polymerization solution or by gelatination. Finally, the beads (matrix) are collected in Step 8 [16].

There is flow vibration nozzle set and concentric nozzle set for microbeads generation and core-shell beads generation respectively. Apart from the nozzle size, beads size is affected by other parameters. Per the operation manual, beads size decreases when (1) Electrostatic potential increases; (2) Gelling ion (Ca^{2+} in this case) concentration increases; (3) Alginate concentration decreases; (4) Alginate viscosity

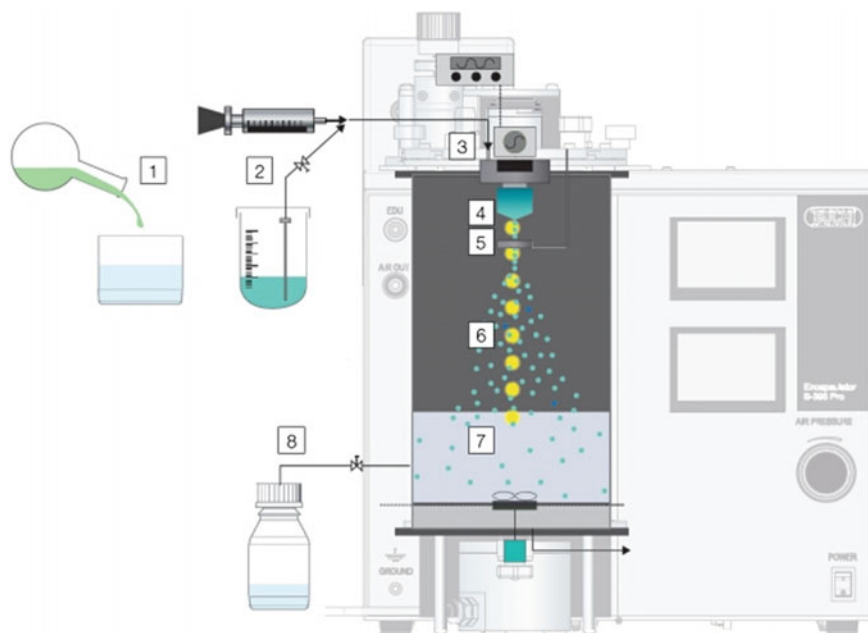
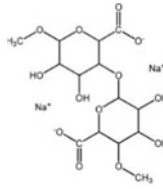


Fig. 5 Mechanism of the encapsulator B-390 and step by step procedure for encapsulation.

decreases and flow rate increases. Among those parameters, the flow rate, electrostatic potential, and viscosity influence the dispersion of the fluid the most, thus affecting the quality of magnetic beads.

3.1.2 Calcium Alginate Gelation Process

Calcium alginate hydrogel bind when covalent bonds form between alginic acids and calcium ions. As described in Fig. 6, alginate is a linear co-polymer composed of two monomeric units. When sodium alginate droplets fall into calcium chloride solution, covalent bonds form between alginic acids and calcium ions. These inter-chain associations can be either permanent or temporary, depending on the concentration of the calcium ions. In this chapter, high concentration of calcium chloride solution is chosen to be optimal and calcium alginate hydrogel beads form permanently in the solution [106, 133]. Figure 6 illustrates the Gelation Processes of the Calcium Alginate.



Ca²⁺

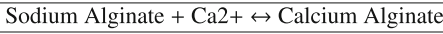
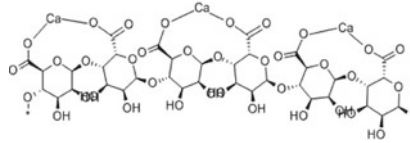


Fig. 6 Gelation processes of the calcium alginate.

3.1.3 Microcapsule Design

The design of microcapsules has been proposed in this chapter and the design rationales is discussed consecutively. The primary design proposed herein is simple in fabrication processes when applied to the locomotion control experiments. The other designs can be utilized to include thermal sensitive properties to the microcapsules, regarding the materials used.

It has been reported that polymer coated magnetic micro/nanoparticles demonstrate excellent *in vitro* and *in vivo* hyperthermia, which is a phenomenon where magnetic nanoparticles oscillate under high frequency alternating magnetic field (HF-AMF) [106, 133] and generate heat. This phenomenon indicates the potential of internal local heating of the microcapsules containing magnetic nanoparticles, hence triggering the hydrophilicity change of the thermosensitive nanogel particles from inside of the microcapsules and increasing the drug release rate.

Briefly, in the proposed design, the calcium alginate core of the microcapsule will contain bovine serum albumin (BSA) as a model drug, carbonyl iron particles for magneto-responsive properties and PNIPAM for thermal sensitive properties. The core will be coated by a layer of chitosan for controlled drug release. This core-shell structured microcapsule design will utilize thermal sensitive property of the material. PNIPAM is a kind of thermal sensitive polymer that changes hydrophilicity when crossing its transition temperature. Therefore, the assumption is made that when the environment temperature rises above the transition point, the PNIPAM hydrogel becomes hydrophobic and dehydrated, this changes the permeability of the microcapsule and increases the release rate of the drug, which is loaded in the core.

Table 2 Specifications of the EMF generator model of the 1D coil system.

D: Diameter T: Thickness L: Length W: Width	
Diameter of the Maxwell coils:	2 * 55.6mm(D) * 11 mm(T)
Diameter of the Helmholtz coils:	2 * 65.6mm(D) * 11 mm(T)
Inter-coils wall:	100 mm(L) * 100 mm(W) * 3.622 mm(T)
Platform:	87.62 mm(L) * 100 mm(W) * 5 mm(T)

3.2 Fabrication of Magnetic Actuation Systems

The proposed coil systems consist of coil supporters, microcapsule container, and platforms. After the models were printed, copper wires of diameter 0.9 mm will be wound to the coil supporters, followed by the assembly of all the components.

3.2.1 One-Dimensional Coil System

The one-dimensional coil system consists of one pair of Helmholtz coils to generate homogeneous magnetic field and one pair of Maxwell coils to generate magnetic gradient field. A simple prototype will be fabricated with a 3D printer and copper wires of diameter 0.9 mm. The printed components will include two identical coil supporters, one particle container and one platform. The wires will be wound on the coil supporters, followed by fixing the supporters to the platform. Table 2 is going to demonstrate sample specifications of the magnetic field generator model of this one-dimensional coil system.

Table 2 is a list of the Specifications of the EMF Generator model of the 1D coil system.

The one-dimensional coil system was connected directly to the power supply. A 5 A–10 A current was fed to the Helmholtz coils and the Maxwell coils. Different magnetic particles were put into the container and an endoscope camera was fixed above the EMA system to record the locomotion of those particles in the container.

3.2.2 Two-Dimensional Coil System

The two-dimensional magnetic field generation system consists of two pairs of Helmholtz coils and two pairs of Maxwell coil. Theoretically, it will be able to control the locomotion of magnetic particles in two dimensions within the Region of interest (ROI). The two-dimensional coil system will be integrated with a current control system to realize current control, hence magnetic field control and finally the locomotion control via programming. The next Section will show the details of the current control system.

Table 3 Specifications of the EMF generator model of the 2D coil system.

D: Diameter T: Thickness	Helmholtz X	Maxwell X	Helmholtz Y	Maxwell Y
D of the core	2 * 36 mm(D)	2 * 40 mm(D)	2 * 90 mm(D)	2 * 50 mm(D)
Inter-coils wall	6 * 68 mm(D) * 2 mm(T)		6 * 160 mm(D) * 2 mm(T)	

Instead of using a platform, this design will include screws and nuts for better stability. The materials for the two-dimensional coil system will be changed from Acrylonitrile butadiene styrene (ABS), which is a very common material for 3D printing, to aluminium. Compared to ABS, aluminium has a higher melting point and better heat transfer ability. Therefore, deformation of the structure can be avoided and changes, for instance, the varying resistance of the coil caused by the heat generated when current passing through, are decreased.

Table 3 is the list of Specifications of the EMF generator model of the 2D coil system.

3.2.3 Power Supply and Current Control System

As proposed, AQMD3620NS DC motor governors receive input power (9–36 V) from the DC power supply and serial signals from the RS485 system to generate respective output power. There are two input points (AI 1 and AI 2) to receive signals for motor speed control and one input point (DE) to receive signals for motor direction control. There are eight system DIP switches for setting of modes, of which the eighth switch defines the control mode. If it is ON, the motor governor is set as a serial communication mode, where each governor is given an address by setting different combinations of the other seven switches. The USB to RS485 converter enables direct communication between the system and the programming environment. Figure 7 sketches the Principle of magnetic actuation over the microcapsules.

3.3 Proposed Design and Materials

The materials going to be used in this following proposed design will include alginic acid sodium salt (Alg, viscosity 15–20 cP in 1% solution) calcium chloride dehydrate ($\text{CaCl}_2 \cdot 2\text{H}_2\text{O}$), and carbonyl iron (CI) powder (BASF). Fabrication with Carbonyl iron ($\text{Fe}(\text{CO})_n$) particles can be irregular shaped dark grey particles with high iron content. Therefore, they are quite sensitive to magnetic fields. It is widely used in the fabrication of Magnetorheological (MR) fluid, coil cores and dietary supplements to discuss in the later stage. Microscale carbonyl iron particles are insoluble in neutral solvents, indicating its stability during transportation. The particles can be added into

sodium alginate solution and the mixture can be injected through the encapsulator and vibrated into micro droplets for gelation processes.

3.3.1 Electromagnetic Actuation (EMA) System

The EMA system mainly consists of two parts: the coil system to generate magnetic field per the current provided and the current control system including the power supply, coil driver based on motor governor, data processor, and routine algorithms.

3.3.2 Coil System

The coil systems are utilized to emanate magnetic fields by the current flux applied through them. With different magnetic coiling parameters, such as the loop diameter and the wire diameter, the emanated field strength and patterns are changed accordingly. In this proposed design, a one-dimensional coil system and a two-dimensional coil system have been proposed for testing. Both consists of Helmholtz pairs and Maxwell pairs are described in the earlier design part.

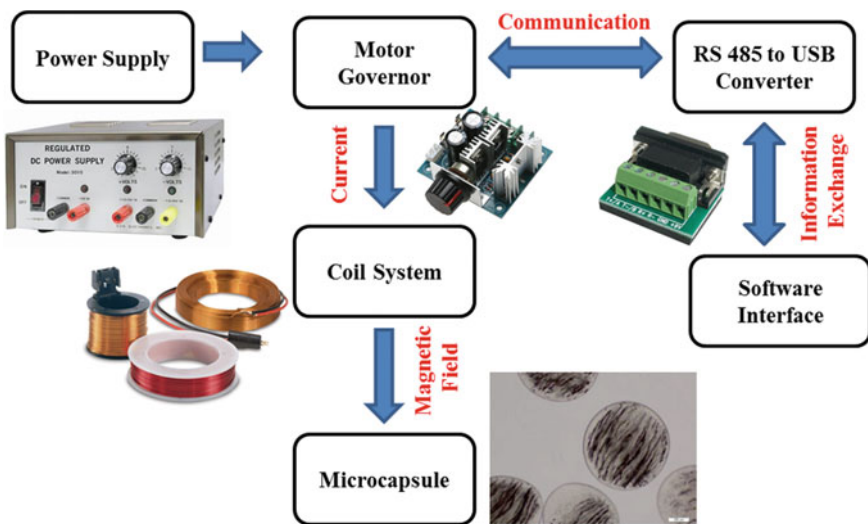


Fig. 7 Principle of magnetic actuation over the microcapsules.

3.3.3 Design Rationale

In general, for the principles, Helmholtz coil pairs generate uniform magnetic field between them along their common axis within the range of interest (ROI), while Maxwell coil pairs emanate constant gradient magnetic field. The Helmholtz coil pairs determine the orientation of the magnetic particles, while the Maxwell coil pairs drive the locomotion of them. With the currents flowing through the coil pairs, the desired magnetic fluxes can be generated. Superposition of the coil pairs generates multidimensional flux vectors.

Helmholtz coil pairs are two parallel identical coils connected to current sources of the same direction and equal flux. The distance between their centers is equal to the coil diameter. According to the Biot-Savart theory, for current flowing through a single wire loop, the magnetic field generated to a point on the axis at a distance x can be derived as in (1):

$$B(x) = \frac{\mu_0 \mu_r I R^2}{2(R^2 + x^2)^{\frac{3}{2}}} \quad (1)$$

where μ_0 is the magnetic permeability of free space and μ_r is the permeability of the environment where the magnetic particle is located. I is the current flowing through the loop and R is the radius of the wire loop. For a point at the center of the axis of the two identical Helmholtz coils with n turns each, the magnetic flux density B_M can be calculated as:

$$\begin{aligned} B_H\left(\frac{R}{2}\right) &= 2 \frac{\mu_0 \mu_r n I R^2}{2\left(R^2 + \left(\frac{R}{2}\right)^2\right)^{\frac{3}{2}}} \\ &= \frac{8}{5\sqrt{5}} \frac{\mu_0 \mu_r n I}{R} \end{aligned} \quad (2)$$

From formula (2), it can be concluded that the uniform magnetic field density is proportional to the current density.

Helmholtz coils are designed to generate uniform magnetic field between them along their common axis. When a magnetic particle is located in the region of interest and not aligned with the direction of the field, torque τ is generated as (3):

$$\tau = V M \times B_H \quad (3)$$

Where V is the volume of the magnetic particle and M is the magnetization of the particle. Therefore, the misaligned particle experiences torque until it is aligned to the direction of the field, where the angle between M and B_M is zero.

Figure 8 is a sketch of the Structure and the Induced Magnetic Field of a Helmholtz Coil Pair.

Similar in structure with the Helmholtz coils, Maxwell coil pairs are parallel identical coils connected to currents with equal flux but opposite directions. As illustrated in Fig. 9, the distance between their centers equals to $\sqrt{3}$ times of the coil diameter.

Figure 9 portrays the Structure and the Induced Magnetic Field of a Maxwell Coil Pair. Maxwell coils usually generate constant gradient magnetic field between them, along not only the axis, but also all directions perpendicular to the axis. The force applied to the magnetic particles inside the region of interest is described as (4):

$$F = V(M \cdot \nabla)B_M \tag{4}$$

Here, V is the volume of the magnetic particle and M is the magnetization. Magnetic flux B_M is described as:

$$B_M = [-0.5g_x, -0.5g_y, g_z] \tag{5}$$

Here, x, y, z are the respective dimensional value of the interested point and g is the magnetic flux gradient calculated as (6):

$$g = \frac{16}{3} \left(\frac{3}{7}\right)^{\frac{5}{2}} \frac{i_m \times n \times \mu_0}{(r_m)^2} \tag{6}$$

Here, μ_0 is the magnetic permeability of free space, n, i_m, r_m are the turns, current, and radius of each coil, respectively. From the formula 6, the gradient magnetic field density is proportional to the current density.

Here in Table 4, we have portrayed few of the significant papers reported from 2009 year and ahead from Prof. Sukho Park Research Group, Chonnam National University, Gwangju, Korea and Prof. Bradley Nelson Research Group, ETH Zurich,

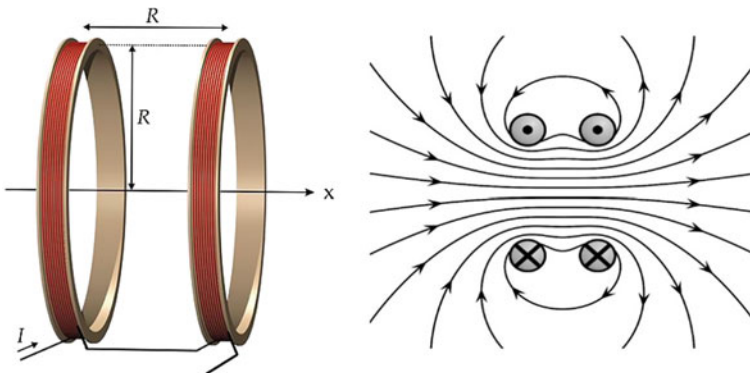


Fig. 8 Structure and the induced magnetic field of a Helmholtz coil pair.

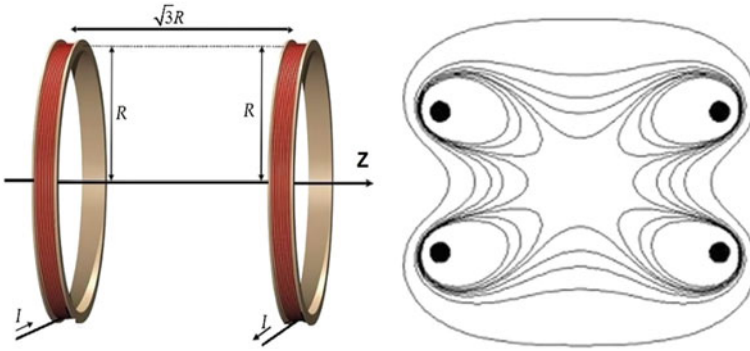


Fig. 9 Structure and the induced magnetic field of a Maxwell coil pair.

Switzerland. This is just to give an initial fragmented idea of the microbots and their design and control strategy in a listed format for ease of the reader, especially who is going to initiate a fresh research in this realm.

Table 4 Brief review of literature in magnetic micro robotics for biomedical applications (Sukho Park research group some selected publications).

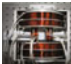

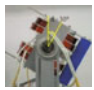




Year	Application	Robot	Size	Material	Magnetic system	Control	ROI	DOF(T+R)	Remarks
2009	Locomotive	Rod	um size	(Permenent Magnet)		Open Loop Camera LabVIEW NI PXI Controller	<35*35mm	2+1(2H2M)	—
2009	Intravascular	Rod	um size (Nd)			OpenLoop... Joystick	D+=60mm	3(1H1M)	Roll-Pitch-RollPosition recognition
2010	Intravascular	Rod	um size (Nd)			OpenLoop... Joystick	<+32mm	3+1(2H2M)	Rotational coil pairs
2010	Intravascular with drilling	Sphere	mm size (Nd Al2O3)			Open Loop	<43mm	3+3(3H2M)	1 Rotational; M coil pair
2010	with ROI developed	Rod	um size (Nd)			NG	NG	2+1(1H1M+1HS+1MS)	More efficient
2013	... with ROI and power developed	Sphere	mm size (Nd Al2O3)			Open Loop	440% Bigger than (4)	3+3(3H1M)	440% bigger WS and 49% less power
2015	Target Therapy	Bacteriobot	5-10um	(CaAlg beads as I. live bacteria)		(same Open Loop LabVIEW NI PXI Controller	(app <35*35mm)	2+1(2H2M)	Bacterial MagHybrid

Table 5 Brief review of literature in magnetic micro robotics for biomedical applications (Bradley Nelson research group some selected publications).




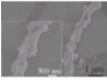
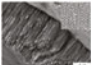
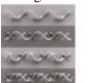
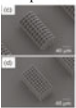
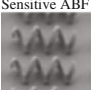
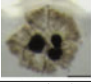

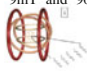

Year	Application	Robot	Size & Material	Magnetic System	ROI	DOF(T+R)	Remarks
2010	5-DOF wireless micromanipulation	Ni Magnetic 	L: 500um	 NG	NG(D<130mm)	3+2C	—
2012	Cell Attachment	Helical micromachine 	L: 8.8um D: 2.0um CSS: 290nm CSL: 900nm	NG	NG	3+3	DLW Thin Film Deposition
2012	Wireless Mag Manipulation	Helical microstructure 	D: 0.5um L: um scale	NA	NA	NA	Cavity
2012	Bio-manipulations	Nanowires 	D: 100nm L: 200nm L: 7um	3H coils	20mm*5mm*2mm 3+3(3H)		Cell tests with microbeads
2013	TDD & Localized manipulations	Flagellum with mastigonemes 	D: 5um CS: 0.7um (SU8/Fe layer)	3H coils	NG	3+3(3H)	Speed depend on Length and Spacing Ratio of the mastigonemes
2013	3D Cell Culture & Targeted Transportation	3D porous niches 	L: arnd 150um D: arnd 73um Pore size: arnd 20um (photocurable polymer Ti & Ni layer)	Minimag (Aeon Scientific, Switzerland)	NG	NG	HEK 293 cells attachment
2014	Triggered Drug Release	Temperature Sensitive ABF 	L: 16um D: 5um (Ti layer DPPC liposomes)	NA	NA	NA	—
2014	TDD & Triggered Release	Encapsulated Magnetic Microbeads 	D: 10um (Alginate)	OctoMag	OctoMag	3+2	Near Infrared Light Triggered Drug Release
2015	Screening	Magnetic Fluorescence ABF 	L: 8um (Ni/Ti layer Photosensitive polymers NIR-797 dye)	9mT and 90Hz 	NG	3+3(3H)	DLW Thin film deposition
2015	TDD & MIS Posterior part of eye	Microtubes 	OD: 300um ID: 125um L: 3.4mm (CoNi layer)	OctoMag 40mT-500mT/ m 1.186T	OctoMag	3+2	In vivo Release Study

Table 4 is a Brief Review of literature in magnetic micro robotics for biomedical applications from Prof. Sukho Park's Research Group (Selected Publications).

Table 5 is a brief review of literature in magnetic micro robotics for biomedical applications from Prof. Bradley Nelson's Research Group (Selected Publications).

4 Electromagnetically Actuated Self-driven Microjet for Biosensing Applications

Artificial micromachines have fascinated researchers around the world for last few decades with the advancements in areas of chemistry, physics, and nanotechnology [70, 109]. Hydrogen peroxide (H_2O_2) has widely been used as fuel to propel tiny motors in the presence of precise electromagnetic motion control. This electromagnetic motion controller can contain different functionalities for diverse applications, including biosensors. Bimetallic nanowires first and more recently microtubular jet engines are two of the most promising candidates to perform useful tasks at the micro/nanoscale. The transport of microparticles in controlled electromagnetic environment into a microfluidic chip was achieved by nanowires and microjets. However, only microtubular jets can self-propel in complex biological samples near EM field. Thus, the controlled transport of cells is significant since it is clearly the next step towards the use of artificial micro/nanomachines in future biomedical applications [101, 127]. In the recent past, efficient isolation of biomaterials such as nucleic acids, proteins, and cancer cells from raw biological samples was achieved by functionalized microjet engines [12]. The rapid development of this research area paves the way for designing new detection platforms and biosensing systems with the need of optical microscopes and tracking methods to measure the speeds of the micro-nanomotors [98].

4.1 Breakthrough and Innovative Aspects

4.1.1 Lab-In-A-Tube

The study of cell behaviors (division time, DNA damage, spindle reorientation, etc.) in 2D confinements represents a pioneering and unique paradigm in cell biology, chemistry, and biotechnology fields. Up to date, most of the studies on cellular behaviors have been explored only on planar 2D patterns, which do not mimic the *in vivo* microenvironment of the cells. The rolled-up microtubes not only serve as 2D microreactors for live cell studies but also as on-chip integrated sensors (optical, electric, or magnetic), which distinguishes the rolled-up nanotechnology from other technologies [38, 108]. In addition, the tubular size is scalable and easily tuned on-demand [69].

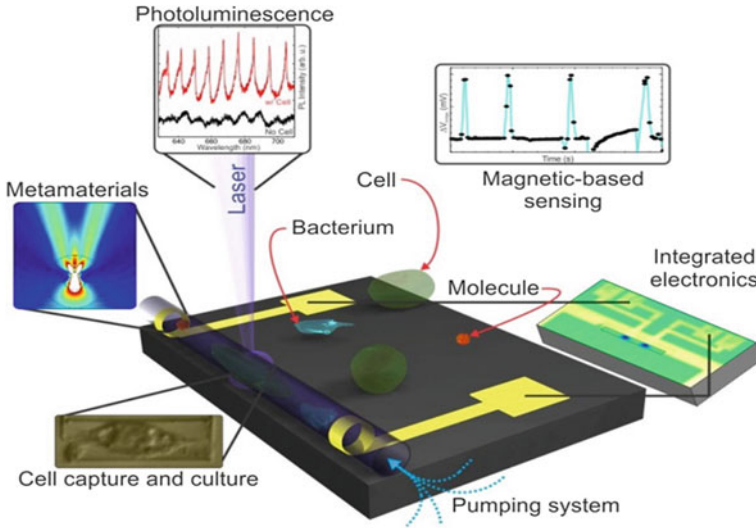


Fig. 10 Lab-in-a-tube device. Capturing and sensing of cells and cellular behaviors [11].

Figure 10 shows a Lab-in-a-tube device capturing and sensing of cells and cellular behaviors [11].

4.1.2 Catalytic Micro/Nanomotors

These tiny machines have demonstrated interesting capabilities to transport cargoes to specific targets in an accurate manner [69]. Despite the increasing number of publications, no reports have clearly proven the biocompatibility of the fuel-machine couple in the presence of EM field [71]. Thus, major future challenges for scientists are (1) effective motion control of micro/nanomotors in vivo; (2) to seek for other biocompatible and clean sources of motion to expand the field of micro/nanomotors to real biomedical and environmental applications. The effective motion control of micro/nanomotors utilizing strong EM field for selective biosensors will surely be of ground-breaking nature [53].

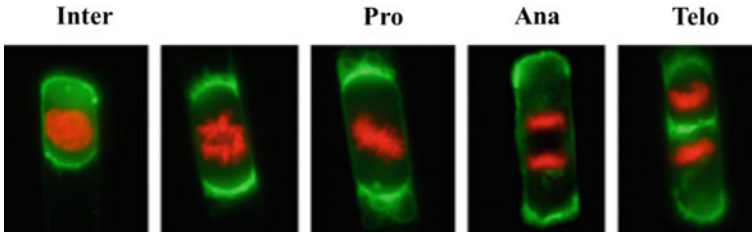


Fig. 11 Different phases of mitosis (cells into tubes) [2].

4.2 *EM Field Motion Control Potential Applications Area: Future Perspectives*

4.2.1 Single Cell Studies into Confined Spaces

• Cell division of animal cells has been studied in detail during the last years (Fig. 11) [18]. However, the relation between cellular morphology and its orientation during division still is mostly under study [20]. Up to now, only flat patterned surfaces have been employed for those studies concluding that the spindle orients in a specific position during the division cycle [57]. There is a great need to bring these investigations into a new concept which resembles the *in vivo* microenvironment that surrounds the cells [5, 72].

(I) Study of Mechanical (Physical) and (Bio) Chemical Stress on DNA Damage

DNA damage and recovery is nowadays a hot topic in cell biology and genetics. DNA damage in cells can be caused by several factors, including chemical or mechanical stress [51, 76]. By scaling the dimensions of the microtubes there is a great need to discriminate the threshold (in microscale size) where the cells sense mechanical stress. In addition, to gain more insight into the influence of external sources for DNA damage [48], there is a need to study several methods of trapping cells [91].

(II) The ability to integrate electrodes within the integrated on-chip tubular structure is a unique feature of the rolled-up nanotechnology. Up to date, off-chip manipulation and sensing of cells have been reported and the glass pipettes containing electrodes are the most common devices to obtain electrical signal from cells. However, those often damage the cells under study. Conclusively, there is a need to establish manipulation, control, and sensing of confined cells by means of electrochemical signals and capacitance difference on-chip. Thereafter, a detailed investigation needed for the magnetic detection of nanoparticles uptake by cells will serve as novel magneto-biosensors completing the Lab-in-a-tube concept [38, 56].

4.2.2 Rolled-Up Microtube as Microreactors for Different Types of Cells and Proteins

The mass production of parallel microtubular structures on-chip will facilitate the separation of different kinds of cells, bacteria, and proteins for bioanalytical and biosensing applications. Magnetically controlled on-chip microbots will simplify several steps of the analytical process since they can separate, isolate and concentrate the desired species (cells). Because of their biocompatibility and transparency, the microtubes will act as microreactors [46, 80] and as sensors for live imaging towards integrative lab-in-a-tube systems [22, 81].

(I) Integration of Optofluidic (Bio) Sensors into Microfluidic Chips

Up to date, rolled-up microtubes have been employed as optofluidic sensors [89], capable of distinguishing different kinds of liquids based on their refractive indexes [24]. Rolled-up SiO_x microtubes [37, 112] can act as optical ring resonators [79] confining light at defined wavelengths in small volumes. The thin walls from rolled-up microtubes can act as optical microcavities since Whispering Gallery Modes (WGMs) [75] are observed in the photoluminescence spectra from the rolled-up nanomembranes. The optical rolled-up resonators can couple the light into the resonant mode of the cross section of the tube. Therefore, changes in the fluid composition or molecules bound to the inner wall surface of the tubes lead to a spectral shift of the resonant modes. As a next step, there is a huge thirst to design microtubes with comparable diameter to the studied cell size (i.e., 15 μm diameter). Once the cells were trapped into the microtubes they sharpened the Quality factor and shifting of the WGMs. It is well known that cancer and normal cell lines have different stiffness and the rigidity and morphology of the cell changes [4] during the division cycle and more drastically during apoptosis [115]. With these optical resonators, there can be an aim to sense these changes optically in confined cells.

Figure 12 demonstrates an optofluidic sensor for detection of cells.

(II) Development of Smart Self-Propelled Micro/Nanomotors For Biosensing, Biomedical, and Environmental Applications

Despite the great success and rapid development of this field, several key questions need to be addressed such as the scalability or the biocompatibility of these tiny machines [15, 123]. How small can the jet engines be and still being self-propelled in fluid? [110] Can they really perform useful bio-related applications? [102, 126] For that purpose, the supreme need is to reduce the toxicity of the fuel down to levels where the cells are viable for long periods. One straightforward method towards this aim has been carried out by warming up the solution to physiological temperatures in which the cells grow. Other sources of motion need to be studied such as light and enzymatic reactions. Moreover, the immunoresponse towards the micro-nanojets will be investigated by incubating the microtubes with macrophages. Understanding on the engulfment process will enable the optimization of the size of the microtubes and material composition to avoid the immunoresponse. These findings will be essential to understand phagocytosis of natural and artificial tubular targets. There is a need to

design microjets which can be functionalized with drugs, proteins, specific antibodies, and DNA on their walls to be employed as biosensors or drug delivery systems [107, 119].

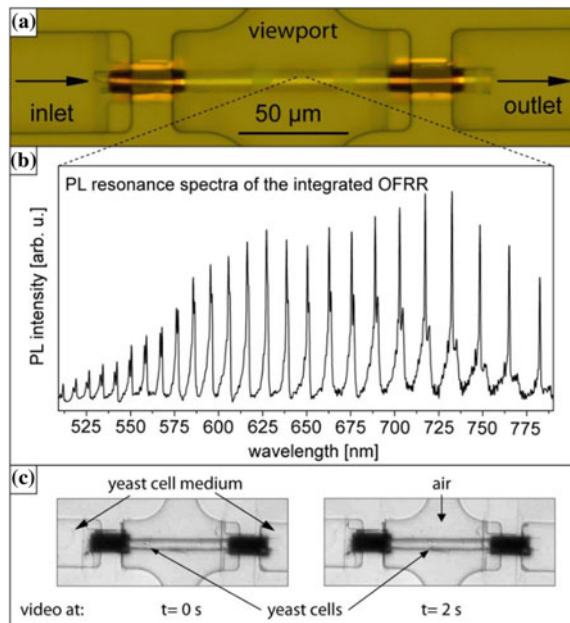
Figure 13 sketches the self-powered microbots remotely guided by a small magnet (B) [1, 87, 100].

4.3 Guidance in Magnetic Actuation

Magnetic robotic microbots or microbubbles which can be controlled by an external magnetic field have been explored as a method for precise and efficient drug delivery. With the increased usage of microbots as a system for drug delivery using ultrasound imaging *in vivo* and using microscopes *in vitro*, there is an interest to develop a tracking and guidance algorithm to locate the position of the microbots during the actuation process. By incorporating real time imaging feedback, better and accurate closed loop robot control, namely visual servoing, can be accomplished.

Typically, the visual servoing algorithm falls into three categories: position-based visual servoing [13], image-based visual servoing [13], and hybrid visual servoing [43, 44]. Since position-based visual servoing calculates the control inputs using the 3D data retrieved from the image features, it is quite sensitive to calibration and reconstruction errors. Both position-based and hybrid methods require the informa-

Fig. 12 Optofluidic sensor for detection of cells.



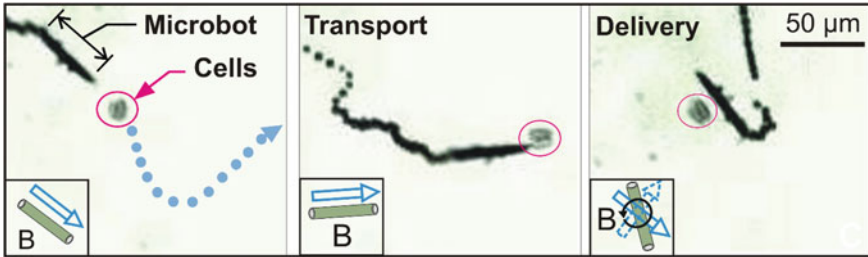


Fig. 13 The self-powered microbots can be remotely guided by a small magnet (B) [1, 87, 100].

tion of the kinematic models of the robots while the current models for surgical robots are complicated and quite inaccurate in constrained surgical environments. Hence, image-based visual servoing is preferable in this application because it can be tailored to utilize only the 2D image features as the feedback to calculate the control inputs while no prior knowledge on robot kinematics is required.

4.4 Control System Design: Future Perspective

In the past decades, several milestones have been attained in the realm of micro/nano scale drug delivery system (as described briefly in the earlier sections) including lab-on-a-chip devices and endoscopic capsules, and for minimally invasive medicines. With the increasing development of micro/nanoscale engineering, it is now possible to batch process nanoscale drug carriers including nanotubes, nanoparticles, and nanowires. A major concern now with the development of this untethered devices *in vivo* is to power them and to control effectively. In this realm, we propose a control strategy for faithful mechanism and manipulation.

Proposed Design and Future Perspectives

Figure 14 is a schematic for proposed magnetic control of self-propelled microjets under ultrasound image guidance. (A) Two sets of electromagnetic coils to be used for generation of controlled magnetic fields [54]. (B) Glass-PDMS hybrid microfluidic device which contains a microchannel using a standard Soft Lithography technique [5, 21]. (C) Microjets move along the magnetic field lines using the propulsion force that is generated due to the ejecting oxygen bubbles from one of their ends [54, 55]. (D) A camera with microscope system will acquire self-propelled microjet real-time images for validation with ultrasound. (E) Ultrasound probe embedded with transducers to acquire images in 3D plane (preferably).

Figure 15 proposed a self-propelled microjets control algorithm. The control system uses the model of self-propelled microjets in a feed forward configuration [54]. Based on the nonlinearity of the system we will use Fuzzy Logic PID Controller or

MPC for better accuracy. The magnetic field strength (B) can be computed as the summation of feed forward controller and MPC. The real-time position tracking algorithm is used to capture ultrasound images (P). The position error $E=P(\text{Reference})-P$ will be used to initiate PID/MPC closed loop control [10].

Proposed Ultrasound-based Tracking of Self-propelled Jets

In contrast to single carrier short duration pulse [10, 95], the proposed technique will use Chirp (Frequency Modulated Signal) coded excitation for better resolution and penetration [39]. Using Chirp as test signal is believed to counteract the long lasting inverse relation (resolution and penetration inversely proportional) trade-off determining accurately noise removal for de-noising in medical US imaging realm [67]. Finally, it is proposed to use Fractional Fourier Transform (FRFT) which is reported to be more flexible for image edge extraction and recognition scenario [116, 131].

Due to the sparsity and multi-resolution property, incorporating wavelet-transform is another novel way which is reported to have emerging potential for speckle noise reduction in 2D and 3D US images [46]. As reported, this will eventually minimize the speckle noise while preserving sharp edges [47, 120].

5 Concluding Remarks and Future Scope

The advances of MRI based diagnosis which falls in the regime of electromagnetically driven actuation is not a new concept. The selling point to use magnetic actuation

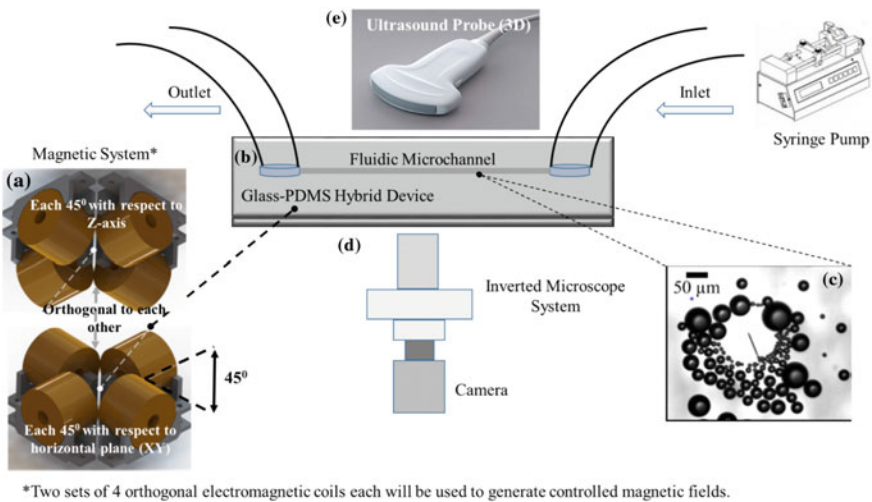


Fig. 14 Schematic for proposed magnetic control of self-propelled microjets under ultrasound image guidance.

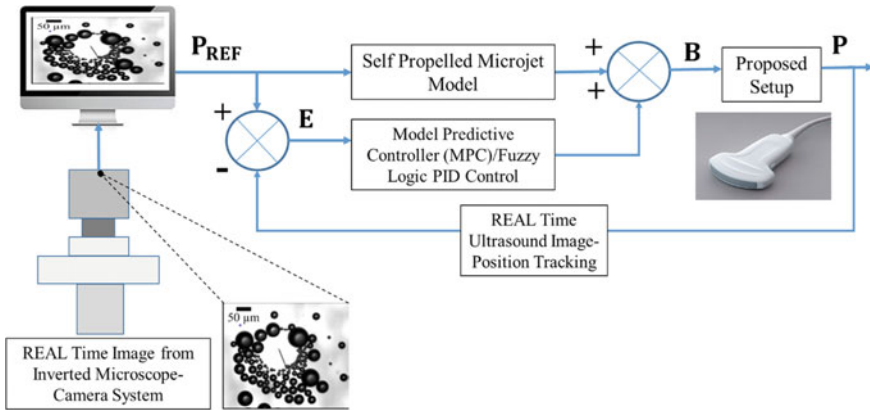


Fig. 15 Proposed self-propelled microjets control algorithm.

for noninvasive drug delivery is multifunctional. The advantages of minimally invasive techniques offer less postoperative pain, less infection, quick recovery time, less hospitalization cost, and overall much higher quality of life. There is no doubt that magnetically driven microbots are going to bring noninvasive drug delivery to a new level but somehow presently the market for commercialization is missing. To dig in more into the problem of functional commercialization there is still a gap in research which needs to be filled beforehand. There are huge number of challenges, e.g., the pH of the media, the heart flow rate and many more to overcome before this Fantastic Voyage turns into reality. Finally, we should be optimistic and constantly work towards building advanced micro motors for biomedical applications when safety is concerned in magnetically driven microbots *in vivo* medical applications.

Acknowledgements This work was in part supported by the Singapore Academic Research Fund under Grant R-397-000-173-133 (Magnetically Actuated Micro Robotics), R-397-000-227-112, and National Natural Science Foundation of China NSFC grant 51405322, NUSRI China Jiangsu Provincial Grant BK20150386 and BE2016077 awarded to Dr. Hongliang Ren.

References

1. Ahmed, Suzanne, et al. 2013. Steering acoustically propelled nanowire motors toward cells in a biologically compatible environment using magnetic fields. *Langmuir* 29 (52): 16113–16118.
2. Alberts, Bruce, et al. 2013. Essential cell biology. Garland Science.
3. Bahaj, A.S., and P.A.B. James. 1993. Characterisation of magnetotactic bacteria using image processing techniques. *IEEE Transactions on Magnetics* 29 (6): 3358–3360.
4. Baker, Erin L., Roger T. Bonnecaze, and Muhammad H. Zaman. 2009. Extracellular matrix stiffness and architecture govern intracellular rheology in cancer. *Biophysical Journal* 97 (4): 1013–1021.

5. Banerjee, Hritwick. 2014. Frequency driven alteration in cellular morphology during ultrasound pulsing in a microfluidic confinement. PhD thesis, Indian Institute of Technology, Gandhinagar.
6. Banerjee, Hritwick and Babji Srinivasan. 2013. Modelling, optimization and control of droplet based microfluidic technology for single-cell high-throughput screening.
7. Berris, M., and M. Shoham. 2006. Febotics-a marriage of fetal surgery and robotics. *Computer Aided Surgery* 11 (4): 175–180.
8. Bose, Nilanjana. 2015. The role of acoustofluidics in targeted drug delivery. *Biomicrofluidics* 9 (5): 052609.
9. Bose, Nilanjana, et al. 2011. The role of cell membrane strain in sonoporation characterised by microfluidic-based single-cell analysis. In *15th International conference on miniaturized systems for chemistry and life sciences*, 1743–1745, Seattle, Washington, USA.
10. Boskma, Klaas Jelmer, Stefano Scheggi and Sarthak Misra. 2016. Closed-loop control of a magnetically-actuated catheter using two-dimensional ultrasound images. In *2016 6th IEEE international conference on biomedical robotics and biomechatronics (BioRob)*, 61–66, IEEE.
11. Burdick, Jared, et al. 2008. Synthetic nanomotors in microchannel networks: Directional microchip motion and controlled manipulation of cargo. *Journal of the American Chemical Society* 130 (26): 8164–8165.
12. Campuzano, S., et al. 2011. Motion-driven sensing and biosensing using electrochemically propelled nanomotors. *Analyst* 136 (22): 4621–4630.
13. Chaumette, Francois. 1998. Potential problems of stability and convergence in image-based and position-based visual servoing. In *The confluence of vision and control*, 66–78.
14. Cheung, Eugene, et al. 2005. A new endoscopic microcapsule robot using beetle inspired microfibrillar adhesives. In *Proceedings, 2005 IEEE/ASME international conference on advanced intelligent mechatronics*, 551–557, IEEE.
15. Chng, Elaine Lay Khim, Guanxia Zhao, and Martin Pumera. 2014. Towards biocompatible nano/microscale machines: self-propelled catalytic nanomotors not exhibiting acute toxicity. *Nanoscale* 6 (4): 2119–2124.
16. Cho, Ah Ra, et al. 2014. Preparation of chitosan-TPP microspheres as resveratrol carriers. In *Journal of Food Science* 79 (4).
17. Collins, James F Jr, et al. 2011. Ophthalmic drug delivery system. US Patent 7,883,031, Feb. 2011.
18. Croce, Carlo M., and George A. Calin. 2005. miRNAs, cancer, and stem cell div. *Cell* 122 (1): 6–7.
19. Croswell, Jennifer M., David F. Ransohoff, and Barnett S. Kramer. 2010. Principles of cancer screening: Lessons from history and study design issues. *Seminars in oncology*, 202–215. Elsevier.
20. Darnell, James E., Harvey Lodish, David Baltimore, et al. 1990. *Molecular cellbiology*. New York: Scientific American Books.
21. Das, Tamal, Tapas K. Maiti, and Suman Chakraborty. 2011. Augmented stressresponsive characteristics of cell lines in narrow confinements. *Integrative Biology* 3 (6): 684–695.
22. Duan, Ruixue, et al. 2013. Lab in a tube: Ultrasensitive detection of microRNAs at the single-cell level and in breast cancer patients using quadratic isothermal amplification. *Journal of the American Chemical Society* 135 (12): 4604–4607.
23. Edd, Jon, et al. 2003. Biomimetic propulsion for a swimming surgical microrobot. In *Proceedings 2003 IEEE/RSJ international conference on intelligent robots and systems (IROS 2003)*, vol. 3, 2583-2588, IEEE.
24. Fan, Xudong. 2011. Optofluidic microsystems for chemical and biological analysis. *Nature Photonics* 5 (10): 591–597.
25. Feringa, Ben L. 2007. The art of building small: From molecular switches to molecular motors. *The Journal of Organic Chemistry* 72 (18): 6635–6652.
26. Flake, Alan W. 2003. Surgery in the human fetus: The future. *The Journal of Physiology* 547 (1): 45–51.

27. Frankel, Richard, Timothy, Williams, and Dennis Bazylinski. 2007. Magnetoerotaxis. In: *Magnetoreception and magnetosomes in bacteria*, 1–24.
28. Garne, E., C. Stoll, and M. Clementi. 2001. Evaluation of prenatal diagnosis of congenital heart diseases by ultrasound: experience from 20 European registries. *Ultrasound in Obstetrics and Gynecology* 17 (5): 386–391.
29. Glass, Paul, Eugene Cheung, and Metin Sitti. 2008. A legged anchoring mechanism for capsule endoscopes using micropatterned adhesives. *IEEE Transactions on Biomedical Engineering* 55 (12): 2759–2767.
30. Glass, Paul, Metin Sitti, and Ragunath Appasamy. 2007. A new biomimetic adhesive for therapeutic capsule endoscope applications in the gastrointestinal tract. *Gastrointestinal Endoscopy* 65 (5): AB91.
31. Glass, Paul, et al. 2008. A motorized anchoring mechanism for a tethered capsule robot using fibrillar adhesives for interventions in the esophagus. In *2nd IEEE RAS & EMBS international conference on biomedical robotics and biomechanics, BioRob*, 758–764, IEEE.
32. Glass, Paul, et al. 2009. A swallowable tethered capsule endoscope for diagnosing Barrett's Esophagus. *Gastrointestinal Endoscopy* 69 (5): AB106.
33. Grady, M.S., et al. 1989. Preliminary experimental investigation of in vivo magnetic manipulation: Results and potential application in hyperthermia. *medical Physics* 16 (2): 263–272.
34. Grady, M.S., et al. 1990. Nonlinear magnetic stereotaxis: Three-dimensional, in vivo remote magnetic manipulation of a small object in canine brain. *Medical Physics* 17 (3): 405–415.
35. Guha, Manalee, et al. 2015. Polymorphisms in CaSR and CLDN14 Genes Associated with Increased Risk of Kidney Stone Disease in Patients from the Eastern Part of India. *PloS one* 10 (6): e0130790.
36. Han, Jiwon, et al. 2016. Hybrid-actuating macrophage-based microrobots for active cancer therapy. *Scientific Reports* 6.
37. Harazim, Stefan M., et al. 2012. Fabrication and applications of large arrays of multifunctional rolled-up SiO/SiO 2 microtubes. *Journal of Materials Chemistry* 22 (7): 2878–2884.
38. Harazim, Stefan M., et al. 2012. Lab-in-a-tube: On-chip integration of glass optofluidic ring resonators for label-free sensing applications. *Lab on a Chip* 12 (15): 2649–2655.
39. Harput, Sevan. 2012. *Use of chirps in medical ultrasound imaging*. University of Leeds.
40. Hoffman, Julien I.E., and Samuel Kaplan. 2002. The incidence of congenital heart disease. *Journal of the American college of cardiology* 39 (12): 1890–1900.
41. Hogers, B., et al. 1995. Intracardiac blood flow patterns related to the yolk sac circulation of the chick embryo. *Circulation Research* 76 (5): 871–877.
42. Holligan, D.L., G.T. Gillies, and J.P. Dailey. 2003. Magnetic guidance of ferrofluidic nanoparticles in an in vitro model of intraocular retinal repair. *Nanotechnology* 14 (6): 661.
43. Hosoda, Koh, Katsuji Igarashi, and Minoru Asada. 1996. Adaptive hybrid visual servoing/force control in unknown environment. In *Proceedings of the 1996 IEEE/RSJ international conference on intelligent robots and systems '96, IROS 96*, vol. 3, 1097–1103, IEEE.
44. Hosoda, Koh, Katsuji Igarashi, and Minoru Asada. 1998. Adaptive hybrid control for visual and force servoing in an unknown environment. *IEEE Robotics & Automation Magazine* 5 (4): 39–43.
45. Hove, Jay R., et al. 2003. Intracardiac fluid forces are an essential epigenetic factor for embryonic cardiogenesis. *Nature* 421 (6919): 172–177.
46. Huang, Gaoshan, et al. 2009. Rolled-up transparent microtubes as two-dimensionally confined culture scaffolds of individual yeast cells. *Lab on a Chip* 9 (2): 263–268.
47. Jaber, Alaa Abdulhady and Robert Bicker. 2014. A simulation of non-stationary signal analysis using wavelet transform based on LabVIEW and Matlab. In *2014 European, Modelling Symposium (EMS)*, 138–144, IEEE.
48. Jackson, Stephen P., and Jiri Bartek. 2009. The DNA-damage response in human biology and disease. *Nature* 461 (7267): 1071–1078.
49. Jeong, Semi, et al. 2011. Enhanced locomotive and drilling microrobot using precessional and gradient magnetic field. *Sensors and Actuators A: Physical* 171 (2): 429–435.

50. Karagozler, Mustafa Emre, et al. 2006. Miniature endoscopic capsule robot using biomimetic micro-patterned adhesives. In *The first IEEE/RAS-EMBS international conference on biomedical robotics and biomechatronics, 2006, BioRob*, 105–111, IEEE.
51. Kasai, Hiroshi. 1997. Analysis of a form of oxidative DNA damage, 8-hydroxy-2-deoxyguanosine, as a marker of cellular oxidative stress during carcinogenesis. *Mutation Research/Reviews in Mutation Research* 387 (3): 147–163.
52. Khalil, Islam S.M., et al. 2013. Characterization and control of biological microrobots. In *Experimental robotics*, 617–631. Springer.
53. Khalil, Islam S.M., et al. 2013. Magnetic control of potential microrobotic drug delivery systems: nanoparticles, magnetotactic bacteria and self-propelled microjets. In *2013 35th annual international conference of the IEEE, engineering in medicine and biology society (EMBC)*, 5299–5302, IEEE.
54. Khalil, Islam S.M., et al. 2013. Three-dimensional closed-loop control of selfpropelled microjets. *Applied Physics Letters* 103 (17): 172404.
55. Khalil, Islam S.M., et al. 2014. The control of self-propelled microjets inside a microchannel with time-varying flow rates. *IEEE Transactions on Robotics* 30 (1): 49–58.
56. Khalil, Islam S.M., et al. 2014. Wireless magnetic-based closed-loop control of self-propelled microjets. *PLoS one* 9 (2): e83053.
57. Kihlman, Bengt A. 1966. Actions of chemicals on dividing cells.
58. Klibanov, Alexander L. 2006. Microbubble contrast agents: targeted ultrasound imaging and ultrasound-assisted drug-delivery applications. *Investigative radiology* 41 (3): 354–362.
59. Kohl, Thomas, et al. 2000. World experience of percutaneous ultrasound-guided balloon valvuloplasty in human fetuses with severe aortic valve obstruction. *The American Journal of Cardiology* 85 (10): 1230–1233.
60. Kosa, Gbor, Moshe Shoham, and Menashe Zaaroor. 2007. Propulsion method for swimming microrobots. *IEEE Transactions on Robotics* 23 (1): 137–150.
61. Kossoff, Eric H., et al. 2002. Kidney stones, carbonic anhydrase inhibitors, and the ketogenic diet. *Epilepsia* 43 (10): 1168–1171.
62. Kristo, Blaine, et al. 2003. Microelectromechanical systems in urology. *Urology* 61 (5): 883–887.
63. Kummer, Michael P., et al. 2010. OctoMag: An electromagnetic system for 5-DOF wireless micromanipulation. *IEEE Transactions on Robotics* 26 (6): 1006–1017.
64. Kwon, Jiwoon, et al. 2006. Friction enhancement via micro-patterned wet elastomer adhesives on small intestinal surfaces. *Biomedical Materials* 1 (4): 216.
65. Latombe, Jean-Claude. 2012. Robot motion planning, vol. 124. Springer Science & Business Media.
66. Leigh, David A. 2016. Genesis of the nanomachines: The 2016 nobel prize in chemistry. *Angewandte Chemie International Edition* 55 (47): 14506–14508.
67. Lizzi, Frederic L., and Ernest J Feleppa. 2000. Image processing and pre-processing for medical ultrasound. In *2000 29th Proceedings applied imagery pattern recognition workshop*, 187–192, IEEE.
68. Lymberis, Andreas. 2010. Micro-nano-biosystems: An overview of European research. *Minimally Invasive Therapy & Allied Technologies* 19 (3): 136–143.
69. Ma, Xing, Kersten Hahn, and Samuel Sanchez. 2015. Catalytic mesoporous Janus nanomotors for active cargo delivery. *Journal of the American Chemical Society* 137 (15): 4976.
70. Magdanz, Veronika, Samuel Sanchez, and Oliver G. Schmidt. 2013. Development of a sperm-flagella Driven Micro-Bio-Ro. *Advanced Materials* 25 (45): 6581–6588.
71. Magdanz, Veronika, et al. 2014. Stimuli-responsive microjets with reconfigurable shape. *Angewandte Chemie International Edition* 53 (10): 2673–2677.
72. Mak, Michael, Cynthia A. Reinhart-King, and David Erickson. 2013. Elucidating mechanical transition effects of invading cancer cells with a subnucleusscaled microfluidic serial dimensional modulation device. *Lab on a Chip* 13 (3): 340–348.
73. Martel, Sylvain, et al. 2007. Automatic navigation of an untethered device in the artery of a living animal using a conventional clinical magnetic resonance imaging system. *Applied Physics Letters* 90 (11): 114105.

74. Mathieu, J.-B., Gilles Beaudoin, and Sylvain Martel. 2006. Method of propulsion of a ferromagnetic core in the cardiovascular system through magnetic gradients generated by an MRI system. *IEEE Transactions on Biomedical Engineering* 53 (2): 292–299.
75. Matsko, Andrey B., and Vladimir S. Ilchenko. 2006. Optical resonators with whispering gallery modes I: basics. *IEEE Journal of Selected Topics in Quantum Electronics* 12 (3): 3.
76. Mayr, Manuel, et al. 2002. Mechanical stress-induced DNA damage and racp38MAPK signal pathways mediate p53-dependent apoptosis in vascular smooth muscle cells. *The FASEB Journal* 16 (11): 1423–1425.
77. McNeil, Robert G., et al. 1995. Functional design features and initial performance characteristics of a magnetic-implant guidance system for stereotactic neurosurgery. *IEEE Transactions on Biomedical Engineering* 42 (8): 793–801.
78. Meecker, David C., et al. 1996. Optimal realization of arbitrary forces in a magnetic stereotaxis system. *IEEE Transactions on Magnetics* 32 (2): 320–328.
79. Mei, Yongfeng, et al. 2008. Versatile approach for integrative and functionalized tubes by strain engineering of nanomembranes on polymers. *Advanced Materials* 20 (21): 4085–4090.
80. Mei, Yongfeng, et al. 2011. Rolled-up nanotech on polymers: from basic perception to self-propelled catalytic microengines. *Chemical Society Reviews* 40 (5): 2109–2119.
81. Min, Xuehong, et al. 2015. Lab in a tube: Sensitive detection of MicroRNAs in urine samples from bladder cancer patients using a single-label DNA probe with AIEgens. *ACS Applied Materials & Interfaces* 7 (30): 16813–16818.
82. Molloy, J.A., et al. 1990. Experimental determination of the force required for insertion of a thermoseed into deep brain tissues. *Annals of Biomedical Engineering* 18 (3): 299–313.
83. Nacev, A., et al. 2010. Magnetic nanoparticle transport within flowing blood and into surrounding tissue. *Nanomedicine* 5 (9): 1459–1466.
84. Nadeau, Caroline, et al. 2015. Intensity-based visual servoing for instrument and tissue tracking in 3D ultrasound volumes. *IEEE Transactions on Automation Science and Engineering* 12 (1): 367–371.
85. Nelson, Bradley J., Ioannis K. Kaliakatsos, and Jake J. Abbott. 2010. Microrobots for minimally invasive medicine. *Annual Review of Biomedical Engineering* 12: 55–85.
86. Pankhurst, Quentin A., et al. 2003. Applications of magnetic nanoparticles in biomedicine. *Journal of Physics D: Applied Physics* 36 (13): R167.
87. Patra, Debabrata, et al. 2013. Intelligent, self-powered, drug delivery systems. *Nanoscale* 5 (4): 1273–1283.
88. Plante, Jean-Sébastien, Lauren M Devita, and Steven Dubowsky. 2007. A road to practical dielectric elastomer actuators based robotics and mechatronics: discrete actuation. In *The 14th international symposium on smart structures and materials & nondestructive evaluation and health monitoring, International Society for Optics and Photonics*, 652406–652406.
89. Psaltis, Demetri, and Stephen R. Quake. 2006. Developing optofluidic technology through the fusion of microfluidics and optics. *Nature* 442 (7101): 381–386.
90. Ren, Liqiang, et al. 2015. A high-throughput acoustic cell sorter. *Lab on a Chip* 15 (19): 3870–3879.
91. Rettig, Jacqueline R. 2005. Large-scale single-cell trapping and imaging using microwell arrays. *Analytical Chemistry* 77 (17): 5628–5634.
92. Roy, Shuvo, et al. 2006. MEMS and neurosurgery. In *BioMEMS and biomedical nanotechnology*, 95–123. Springer.
93. Rubinstein, Leslie. 2000. A practical nanorobot for treatment of various medical problems. In *Draft paper for the 8th foresight conference on molecular nanotechnology*, Bethesda, Maryland.
94. Saettone, Marco Fabrizio. 2002. Progress and problems in ophthalmic drug delivery. *Business Briefing: Pharmatech* 1: 167–71.
95. Sánchez, Alonso, et al. 2014. Magnetic control of self-propelled microjets under ultrasound image guidance. In *2014 5th IEEE RAS & EMBS international conference on biomedical robotics and biomechatronics*, 169–74, IEEE.
96. Sánchez, Samuel. Chemical nanomachines as active drug nanovehicles.

97. Samuel Sánchez. Hybrid micro and nanoBots as future active drug carriers.
98. Sánchez, Samuel, Lluís Soler, and Jaideep Katuri. 2015. Chemically powered micro-and nanomotors. *Angewandte Chemie International Edition* 54 (5): 1414–1444.
99. Sanchez, Samuel, et al. 2010. Dynamics of biocatalytic microengines mediated by variable friction control. *Journal of the American Chemical Society* 132 (38): 13144–13145.
100. Sanchez, Samuel, et al. 2010. Microbots swimming in the flowing streams of microfluidic channels. *Journal of the American Chemical Society* 133 (4): 701–703.
101. Sanchez, Samuel, et al. 2011. Controlled manipulation of multiple cells using catalytic microbots. *Chemical Communications* 47 (2): 698–700.
102. Sánchez, Samuel, et al. 2014. Tubular micro-nanorobots: smart design for biorelated applications. In *Small-scale robotics. From nano-to-millimeter- sized robotic systems and applications*, 16–27. Springer.
103. Satterfield, Charles N, Ralph L Wentworth, and Sterge T Demetriades. 1953. The viscosity of vapor mixtures of hydrogen peroxide and water. Technical Report, MASSACHUSETTS INST OF TECH CAMBRIDGE HYDROGEN PEROXIDE LABS.
104. Seiffert, Sebastian. 2013. Small but smart: Sensitive microgel capsules. *Angewandte Chemie International Edition* 52 (44): 11462–11468.
105. Senyei, Andrew, Kenneth Widder, and George Czerlinski. 1978. Magnetic guidance of drug-carrying microspheres. *Journal of Applied Physics* 49 (6): 3578–3583.
106. Shi, Jun, Natalia M Alves, and Joao F Mano. 2008. Chitosan coated alginate beads containing poly (N-isopropylacrylamide) for dual-stimuli-responsive drug release. *Journal of Biomedical Materials Research Part B: Applied Biomaterials* 84 (2): 595–603.
107. Sitti, Metin, et al. 2015. Biomedical applications of untethered mobile milli/microbots. *Proceedings of the IEEE* 103 (2): 205–224.
108. Smith, Elliot J., et al. 2010. Lab-in-a-tube: detection of individual mouse cells for analysis in flexible split-wall microtube resonator sensors. *Nano Letters* 11 (10): 4037–4042.
109. Soler, Lluís, et al. 2013. Self-propelled micromotors for cleaning polluted water. *Acs Nano* 7 (11): 9611.
110. Solovev, Alexander A., et al. 2009. Catalytic microtubular jet engines self-propelled by accumulated gas bubbles. *Small* 5 (14): 1688–1692.
111. Solovev, Alexander A., et al. 2010. Magnetic control of tubular catalytic microbots for the transport, assembly, and delivery of micro-objects. *Advanced Functional Materials* 20 (15): 2430–2435.
112. Songmuang, R., et al. 2007. From rolled-up Si microtubes to SiO_x/Si optical ring resonators. *Microelectronic Engineering* 84 (5): 1427–1430.
113. Steinberger, Bernhard, et al. 1994. Movement of magnetic bacteria in time-varying magnetic fields. *Journal of Fluid Mechanics* 273: 189–211.
114. Stroumbakis, Nicholas, et al. 1997. Clinical significance of repeat sextant biopsies in prostate cancer patients. *Urology* 49 (3): 113–118.
115. Suresh, Subra. 2007. Biomechanics and biophysics of cancer cells. *Acta Materialia* 55 (12): 3989–4014.
116. Tao, Ran, Lin Qi, and Yue Wang. 2004. *Theory and applications of the fractional Fourier transform*. Beijing: Publisher of Tsinghua University.
117. Temel, Fatma Zeynep and Serhat Yesilyurt. 2011. Magnetically actuated micro swimming of bio-inspired robots in mini channels. In *2011 IEEE international conference on mechatronics (ICM)*, 342–347, IEEE.
118. Tobita, Kimimasa, and Bradley B Keller. 2000. Right and left ventricular wall deformation patterns in normal and left heart hypoplasia chick embryos. *American Journal of Physiology-Heart and Circulatory Physiology* 279 (3): H959–H969.
119. Trewyn, Brian G., et al. 2007. Mesoporous silica nanoparticle based controlled release, drug delivery, and biosensor systems. *Chemical Communications* 31: 3236–3245.
120. Uddin, Muhammad Shahin, et al. 2016. Speckle-reduction algorithm for ultrasound images in complex wavelet domain using genetic algorithm-based mixture model. *Applied Optics* 55 (15): 4024–4035.

121. Unger, Bertram J., et al. 2002. Virtual peg-in-hole performance using a 6-dof magnetic levitation haptic device: Comparison with real forces and with visual guidance alone. In *Proceedings, 10th symposium on haptic interfaces for virtual environment and teleoperator systems, HAPTICS*, 263–270, IEEE.
122. Van, Mien, et al. 2016. Fault diagnosis in image-based visual servoing with eye-in-hand configurations using Kalman filter. *IEEE Transactions on Industrial Informatics* 12 (6): 1998–2007.
123. Wang, Joseph, and Wei Gao. 2012. Nano/microscale motors: biomedical opportunities and challenges. *ACS nano* 6 (7): 5745–5751.
124. Wang, Joseph, and Kalayil Manian Manesh. 2010. Motion control at the nanoscale. *Small* 6 (3): 338–345.
125. Wu, Keyu, Liao Wu, and Hongliang Ren. 2014. An image based targeting method to guide a tentacle-like curvilinear concentric tube robot. In *2014 IEEE international conference on robotics and biomimetics (ROBIO)*, 386–391, IEEE.
126. Yingjie, Wu, et al. 2012. Autonomous movement of controllable assembled Janus capsule motors. *ACS Nano* 6 (12): 10910–10916.
127. Xi, Wang, et al. 2013. Rolled-up magnetic microdrillers: towards remotely controlled minimally invasive surgery. *Nanoscale* 5 (4): 1294–1297.
128. Yang, Quanhe, et al. 2006. Racial differences in infant mortality attributable to birth defects in the United States, 1989–2002. *Birth Defects Research Part A: Clinical and Molecular Teratology* 76 (10): 706–713.
129. Yesin, K Berk, Karl Vollmers, and Bradley J Nelson. 2006. Modeling and control of untethered biomicrorobots in a fluidic environment using electromagnetic fields. *The International Journal of Robotics Research* 25 (5–6): 527–536.
130. Zhang, Li, et al. 2010. Controlled propulsion and cargo transport of rotating nickel nanowires near a patterned solid surface. *ACS Nano* 4 (10): 6228–6234.
131. Zhang, Xinghui, et al. 2015. Alpha stable distribution based morphological filter for bearing and gear fault diagnosis in nuclear power plant. *Science and Technology of Nuclear Installations*.
132. Zhou, Yue, et al. 2013. Robotics in natural orifice transluminal endoscopic surgery. *Journal of Mechanics in Medicine and Biology* 13 (02): 1350044.
133. Zhu, Xiaoli, et al. 2012. Preparation and characterization of nanosized P (NIPAMMBA) hydrogel particles and adsorption of bovine serum albumin on their surface. *Nanoscale Research Letters* 7 (1): 519.